

**Corrosion of an aluminum alloy chilled in flowing seawater
and the effect of cathodic prevention**

Akihiro Yabuki^{*}, David T. Yasunaga^a, Toshihiro Shibutani^b, Koichi Shinkai^b

^{}Graduate School of Engineering, Hiroshima University*

1-4-1 Kagamiyama, Higashi-hiroshima, 739-8527 Japan

ayabuki@hiroshima-u.ac.jp

^aTechnical Development Group, KOBE STEEL, LTD

9-12, Kita-Shinagawa 5-chome, Shinagawa-ku, TOKYO, 141-0001 JAPAN

^bMachinery & Engineering Company, KOBE STEEL, LTD

3-1, Shinhama 2-chome, Arai, Takasago, Hyogo 676-8670 Japan

A new type of jet-in-slit testing apparatus for a specimen, chilled with a peltier element, was developed to investigate corrosion on the heat transfer surface of an aluminum alloy heat exchanger, in contact with a liquefaction gas at cryogenic temperature and in flowing seawater. The specimen can be chilled, even under flowing conditions, using this apparatus. Corrosion tests and polarization measurements of a specimen chilled by a peltier element were carried out in flowing seawater at various temperatures. The effect of chilling a specimen was equivalent to the effect achieved for a test in solution at a lower temperature. The process was dependent on a passive film, formed on the surface of the aluminum alloy specimen, as evidenced by polarization measurements. The extent of corrosion damage increased with increasing temperature of the solution, and showed maximum damage at high temperature. At high temperatures, erosion-corrosion was found at the central part of the specimen, but the effect of flow was negligible at low temperature. Corrosion tests for a cathodically polarized specimen were conducted under flowing conditions. Corrosion damage was accelerated by cathodic polarization at lower temperatures.

Keywords: erosion-corrosion, aluminum, peltier element, cathodic corrosion

1 Introduction

Aluminum alloys are used as heat exchangers in air separation plants that are operated at cryogenic temperature, including ethylene plants, liquefaction gas plants and gas vaporization plants, because of their excellent mechanical properties at lower

temperature, high heat transfer properties and economical performance. Damage by corrosion is not apparent in an air separation plant, since the fluid processed in the plant is relatively clean. Heat sources such as air, hot water and seawater are used in a gas vaporization plant depending on the environment and the scale of the plant. Seawater is used as a heat source in a large-scale gas vaporization plant in close proximity to the coast, and corrosion that occurs on the surface of the seawater side of the heat exchanger in the plant must be prevented.

In general, a passive film, which is formed on the surface of aluminum alloys prevents corrosion damage by forming a barrier contact between the bare aluminum metal and the corrosive environment. An aluminum-magnesium alloy having relatively good anti-corrosion properties is used for this purpose, but such a passive film can be disrupted by attack by chloride ions in seawater, leading to corrosion damage. Pitting corrosion occurs where the solution is stagnant and erosion-corrosion occurs due to shear stress and turbulence generated when the flow velocity is high [1]. A film formed on the surface of aluminum alloys greatly depends on, not only the composition of the alloys, but also on environmental factors such as temperature and the type of ion in the solution. The formation of a film is particularly sensitive to temperature, and a boemite film is formed at temperatures higher than 50°C [2]. It has been reported that cathodic protection of aluminum alloys can be effective [3-8], however, corrosion damage might occur during the cathodic protection operation, in which alkali species can be generated near the surface of an aluminum alloy [9].

In this study, the corrosion behavior of a hot water vaporizer, used as a heat exchanger in a gas liquefaction plant, where seawater is used, was investigated. One feature of the exchanger in the plant is that the surface at the seawater side of the

material is chilled to near the freezing point of seawater and seawater flows over the surface at a high velocity. Because of this, the corrosion occurring in the heat exchanger would be expected to have the following characteristics: (1) Corrosion might occur since it appears to be difficult to form a protective film against corrosion at lower temperatures. (2) Unusual corrosion might occur because of the temperature distribution inside the aluminum alloys as a heat transfer material. (3) Corrosion might be accelerated by flowing effects. In addition, (4) Corrosion might occur by cathodic prevention, if such a process is applied.

In order to clarify these concerns, a new type of jet-in-slit testing apparatus for a specimen chilled by a peltier element was developed, and corrosion tests and polarization measurements were carried out at various temperatures in artificial seawater under flowing conditions. The effect of chilling the specimen on corrosion was investigated. The surface appearance and cross-sectional profiles of a specimen after the test were observed and corrosion tests at various flow velocities were conducted to define the type of corrosion that occurs. Corrosion tests on a cathodically polarized specimen were conducted under flowing seawater at various temperatures to evaluate the effect of cathodic prevention.

2 Experimental

2.1 Testing apparatus

Fig. 1 shows a schematic diagram of the developed jet-in-slit testing apparatus for a specimen chilled by a peltier element. The test solution was injected towards the

surface of the specimen from a 16 mm diameter nozzle with a nozzle mouse having a 1.6 mm inner diameter, and it flowed radially in a 0.4 mm gap to reproduce erosion-corrosion due to intense shear stress and turbulence [1]. A peltier element (STS Co. Ltd., T151-60-127S) was used to chill the specimen. A specimen was set on the cooling side of the peltier element, and a water cooling block made of aluminum was installed the heating side of a peltier element. Silicon grease was applied between the peltier element, the specimen and the water cooling block. The temperature of the cooling side of the peltier element was monitored by means of a thermocouple.

Aluminum alloy A5083 was used as the test material. The chemical composition of the material are indicated in Table 1. The dimension of the specimen was 16 mm in diameter and 5 mm in thickness. The specimen was polished with #2000 emery paper, and then ultrasonically cleaned in acetone to remove fat. The solution for the corrosion test was artificial seawater (Yashima Pure Chemicals Co.,Ltd.). The temperature of the solution was maintained between 5 and 45°C with a heater and cooler. Air saturation was performed to maintain the concentration of dissolved oxygen in the test solution. All corrosion tests were conducted under flowing conditions for 20 h. The flow rate of the test solution was set in 0.05 to 0.6 L min⁻¹, equivalent to a flow velocity of 0.4 to 5 m s⁻¹ at the nozzle mouse.

2.2 Evaluation of corrosion

Mass loss of the specimen, the difference between the mass of the specimen before and after the test, was adopted to evaluate corrosion properties. The surface of the specimen was observed after the test. The cross-sectional profile of the specimen

before and after the test was measured using a surface roughness meter, filled with a needle tip with a radius of 5 μm , to evaluate local damage to the specimen by corrosion.

2.3 Polarization measurements

Polarization curves were obtained under flowing conditions. A platinum electrode and a Ag/AgCl electrode were used as the counter and reference electrodes. Measurements were started after exposing the specimen to a flowing solution for 1 h to achieve a steady-state surface for the specimen. The corrosion potential of the specimen was measured to confirm this fact before starting the polarization measurements. Cathodic and anodic polarization curves were measured, respectively, with a scanning rate of 20 mV min^{-1} using a potentiostat (HA-501G, Hokuto Denko Co.,Ltd.). Measurement data was input into a personal computer through a GPIB interface. Corrosion tests under flowing solution conditions for a specimen polarized at a constant potential were conducted using this system.

3 Results and discussion

3.1 Chilling ability of a peltier element

The chilling ability of the peltier element in this apparatus was examined. This was evaluated without installing a specimen on the peltier element. The temperature of the cooling side surface of the peltier element after supplying power is shown in Fig. 2. The temperature of the surface of the element decreased substantially after

supplying power and, after approximately 100 sec, it reached a steady-state temperature of -28°C . In observing the surface of the elements, some ice was found on it.

The temperature of the element surface under flowing conditions was measured by installing the specimen on the elements. The relationship between the temperature of the surface of the peltier element and flow rate is shown in Fig. 3. The temperature of the test solution was 30°C . When the flow rate was 0.02 L min^{-1} , the temperature of the surface of the peltier element was nearly 0°C , and the temperature increased with increasing flow rate. It reached a constant value of 10°C at flow rates higher than 0.2 L min^{-1} . Compared to the result without installing a specimen, the temperature of the surface of the peltier element increased, however, it was lower than the temperature of the solution. This indicates that the peltier element can be used to chill a specimen, even under flowing conditions in this apparatus. In addition, the heat transfer rate from the solution to the peltier element became constant at more than 0.2 L min^{-1} . As the flow rate was adjusted to more than 0.2 L min^{-1} , the effect of flow rate, namely flow velocity, on the corrosion of the chilled specimen could be examined.

3.2 Effect of chilling by a peltier element

Corrosion behavior of the specimen chilled and without chilling by the peltier element was compared. The temperature of the solution is an important factor in evaluating the effect of chilling, and the corrosion test was accordingly carried out at various temperatures of test solution. Fig. 4 shows the mass loss of specimens without chilling and chilled by the peltier element, under flowing solution conditions at various temperatures at a flow rate of 0.32 L min^{-1} . The 2 mg mass loss at 20 h corresponded

to an average corrosion rate of 1.6 mm y^{-1} . Although the mass loss of a specimen without chilling was less than 0.1 mg at 5°C and 10°C , it increased with increasing solution temperature. It decreased in an opposite manner at a temperature higher than 35°C . The maximum mass loss was 1.6 mg, and the corrosion rate exceeded 1 mm y^{-1} . The corrosion of a specimen chilled by the peltier element showed the same behavior as the specimen without chilling, but the mass loss at lower temperatures was larger, and the temperature for achieving maximum mass loss was 40°C . This indicates that the effect of chilling by the peltier element was apparently the same as the corrosion behavior in a solution that was 5°C lower than the temperature of the solution in this apparatus. No unusual corrosion by chilling a specimen was observed. The effect of temperature will be discussed below.

Polarization curves of specimens with and without chilling under a flowing solution at 10, 20 and 30°C are shown in Fig. 5. Before starting the measurement, a specimen was exposed to a flowing solution, and it was confirmed that the corrosion potential measured for each specimen became constant within 1 h. Therefore, the curves indicate the characteristics of a stable surface. The corrosion potential of a specimen without chilling by the peltier element became high with decreasing temperature of the solution (Fig. 5 (a)). A passive region was observed in anode polarization curve, and the current density of these specimens increased rapidly at -0.65 V . This was due to the destruction of the passive film, because considerable pitting was observed on the surface of the specimen after the anodic polarization measurement. The current density in the passive region decreased with decreasing solution temperature. This shows that the passive film formed at a lower temperature has excellent corrosion resistance. No differences were found in the cathodic polarization curves. The

corrosion potential of a specimen chilled by the peltier element as shown in Fig. 5 (b) was higher than that for a specimen without chilling. The passive region became smaller compared to a specimen without chilling, however, the cathodic polarization curves were not changed. This confirms that the effect of chilling by the peltier element mainly affected the anodic reaction responsible for the formation of a passive film.

3.3 Effect of temperature and flow rate

The surface appearance and cross-sectional profile of a specimen without chilling after a 20 h corrosion test under flowing solution conditions at 10, 20 and 30°C are shown in Fig. 6. The polish lines remained on the surface of the specimen tested at 10°C, and the entire surface of the specimen showed a metallic luster. The central part of the specimen tested at 20°C was damaged slightly and bare metal could be observed, although a gray film was formed at the periphery. This damage was due to the impingement of the solution in the apparatus¹⁾. The surface of the specimen tested at 30°C was similar as that at 20°C, but the damaged area was larger and the damage depth was approximately 5 µm at the central portion. The surface appearance and profile of the chilled specimen were similar to the result for a specimen without chilling at each temperature tested.

Relationships between the mass loss of a chilled specimen and the flow rate of the solution at 10 and 30°C are shown in Fig. 7. The mass loss of a specimen tested at 30°C increased with increasing flow rate, and rapidly increased at a flow rate of approximately 0.2 L min⁻¹. This corresponded to a flow velocity of 1.6 m s⁻¹ at the

nozzle mouse in the apparatus, which was to be the breakaway velocity [10]. On the other hand, the mass loss of the specimen tested at 10°C was very low, almost constant, even when the flow rate was increased. Taking the results of surface appearance and the damage profile into account, it can be concluded that erosion-corrosion occurs for the specimen tested under flowing solution conditions at 30°C. The corrosion rate of a specimen tested at 10°C was very low and is not affected by the flow of the solution.

3.4 Effect of cathodic polarization

In order to elucidate the effect of cathodic polarization, a corrosion test of a specimen polarized cathodically without chilling was carried out in a flowing solution of 10°C at flow rate of 0.32 L min⁻¹. The mass loss of a specimen polarized at a potential of -1000, -1100 and -1200 mV is shown in Fig. 8. The mass loss of a specimen tested at the corrosion potential (E_{corr}) without polarization is shown in the figure as a reference. The corrosion potential of the specimen was -852 mV at the end of the test. A cathodically polarized specimen was damaged extensively, and the mass loss of a specimen polarized at -1000 mV was the largest, more than 10 times the mass loss of the non-polarized specimen.

Mass loss of a specimen polarized at -1000 mV without chilling at various temperatures is shown in Fig. 9. Corrosion tests were conducted under flowing solution conditions at a flow rate of 0.32 L min⁻¹. The mass loss of a non-polarized specimen, which was shown in Fig. 4, is shown as a dotted line in the figure as a reference. The mass loss of a polarized specimen was larger at lower temperatures, and reached a maximum at 20°C. In comparing the mass loss of a polarized specimen

with a non-polarized specimen, the mass loss of a polarized specimen was larger at temperatures lower than 25°C. The reason for why mass loss reached a maximum at 20°C appears to be related to the passive film formed on the surface, since the film condition differs between at 10 and 30°C as indicated in Fig. 6 and Fig. 7. A passive film might be not formed by cathodic polarization at lower temperatures and, as a result, the mass loss of a polarized specimen would be expected to be increased. On the other hand, the mass loss of a polarized specimen at 30°C did not increase, since the film had already been disrupted by turbulence occurring in the flow.

In order to evaluate the state of the passive film of a polarized specimen at lower temperature, the following test was conducted. A specimen polarized using -1000 mV of surface potential, was exposed to flowing solution conditions for 1 h. A polarization curve was then measured in the direction of the potential to confirm a passive region in the curve. The polarization curve measured for a polarized specimen exposed to a flowing solution of 20°C at a flow rate of 0.32 L min⁻¹ is shown in Fig. 10. The polarization curve of a non-polarized specimen is shown in the figure as a reference. Although a passive region in anodic polarization curve was recognized in a non-polarized specimen, a similar region was not found in a polarized specimen. This confirms that a passive film forms on a cathodically polarized surface with difficulty at lower temperatures. Compared to these curves, the cathodic current of a polarized specimen was larger. This indicates that the anodic reaction was not only accelerated but that the cathodic reaction was also accelerated, since a passive film is difficult to form by cathodic polarization.

These results suggest that cathodic protection for an aluminum alloy is not effective under flowing seawater near the freezing point, and might lead to more extensive

corrosion. If cathodic prevention were to be applied at lower temperatures in a seawater environment, the conditions must be carefully chosen, since the characteristics of the passive film will depend on the composition of the aluminum alloy and the type of ions present.

4 Conclusions

A new type of jet-in-slit testing apparatus for a specimen chilled with a peltier element was developed. Corrosion tests and polarization measurements for an aluminum alloy were carried out in flowing artificial seawater, and the following results were obtained.

1. The effect of chilling by the peltier element was apparently the same as the corrosion behavior in a solution 5°C lower than the temperature of the solution in this apparatus. No unusual corrosion by chilling the specimen was found.
2. As the temperature of the solution became lower, corrosion damage to the specimen decreased. This was caused by the formation of an excellent passive film against corrosion at lower temperatures.
3. Corrosion damage to an aluminum alloy increased with increasing flow velocity of seawater at 30°C, and a breakaway velocity was recognized, therefore, damage occurring at 30°C is “Erosion-corrosion”. The extent of corrosion damage at lower temperatures was very low, and it was not affected by flow.
4. A corrosion test of a specimen polarized at -1000 mV was carried out under flowing seawater, and the corrosion was accelerated at temperatures below 25°C. This is because a passive film could not be formed on a specimen by cathodic polarization.

References

- [1] M. Matsumura, Y. Oka, S. Okumoto, H. Furuya: *ASTM STP 866*, **1985**, 358.
- [2] W. Vedder, D.A. Vermilyea: *Trans. Faraday Soc.*, **1969**, 65, 561.
- [3] G.W. Akimow: *Tr. of Central Aero-Hydrog. Inst.*, **1931**, 70, 1.
- [4] P. Brenner: *Z. Metallk.*, **1937**, 29, 334.
- [5] W. Geller: *Z. Metallk.*, **1939**, 31, 365.
- [6] H. Kostron: *Aluminium*, **1941**, 23, 195.
- [7] F.C. Althof, S. Rastock, *Korrosion und Metallschutz*, **1940**, 16, 217.
- [8] W. Bungardt: *Z. Metallk.*, **1940**, 32, 363.
- [9] G. Ito: *Journal of Japan Institute of Light Metals*, **1954**, 4, 91.
- [10] B.C. Syrett: *Corrosion*, **1976**, 32, 242.

Captions

Fig. 1. A jet-in-slit testing apparatus for a specimen chilled with a peltier element.

Fig. 2. Temperature of the cooling side of the surface of a peltier element after supplying power. No specimen is installed on the peltier element.

Fig. 3. Temperature of the surface of a peltier element in a flowing solution at 30°C at various flow rates.

Fig. 4. Relationship between solution temperature and mass loss of a specimen without chilling and chilled by a peltier element under flowing conditions at a flow rate of 0.32 L min^{-1} .

Fig. 5. Polarization curves for a specimen under a flowing solution at a flow rate of 0.32 L min^{-1} at various temperatures; (a) without chilling, (b) chilled by a peltier element.

Fig. 6. Surface appearance and cross-sectional profile of a specimen tested without chilling for 20 h at various temperatures at a solution at flow rate of 0.32 L min^{-1} .

Fig. 7. Relationship between the flow rate of the solution and mass loss of a specimen chilled by a peltier element after a 20 h test in a solution at 10°C and 30°C .

Fig. 8. Mass loss of a specimen polarized cathodically without chilling under a flowing solution at a flow rate of 0.32 L min^{-1} at 10°C .

Fig. 9. Relationship between solution temperature and mass loss of a specimen polarized cathodically at -1000 mV vs. Ag/AgCl without chilling under a flowing solution at a flow rate of 0.32 L min^{-1} . Dotted line is for a non-polarized specimen, as shown in figure 4.

Fig. 10. Polarization curve measured after exposing a specimen polarized at -1000 mV

vs. Ag/AgCl to a flowing solution at 20°C at a flow rate of 0.32 L min⁻¹ for 1 h.

Polarization curve for a non-polarized specimen is shown as a reference.

Table 1 Chemical composition of aluminum alloy 5083 (mass%).

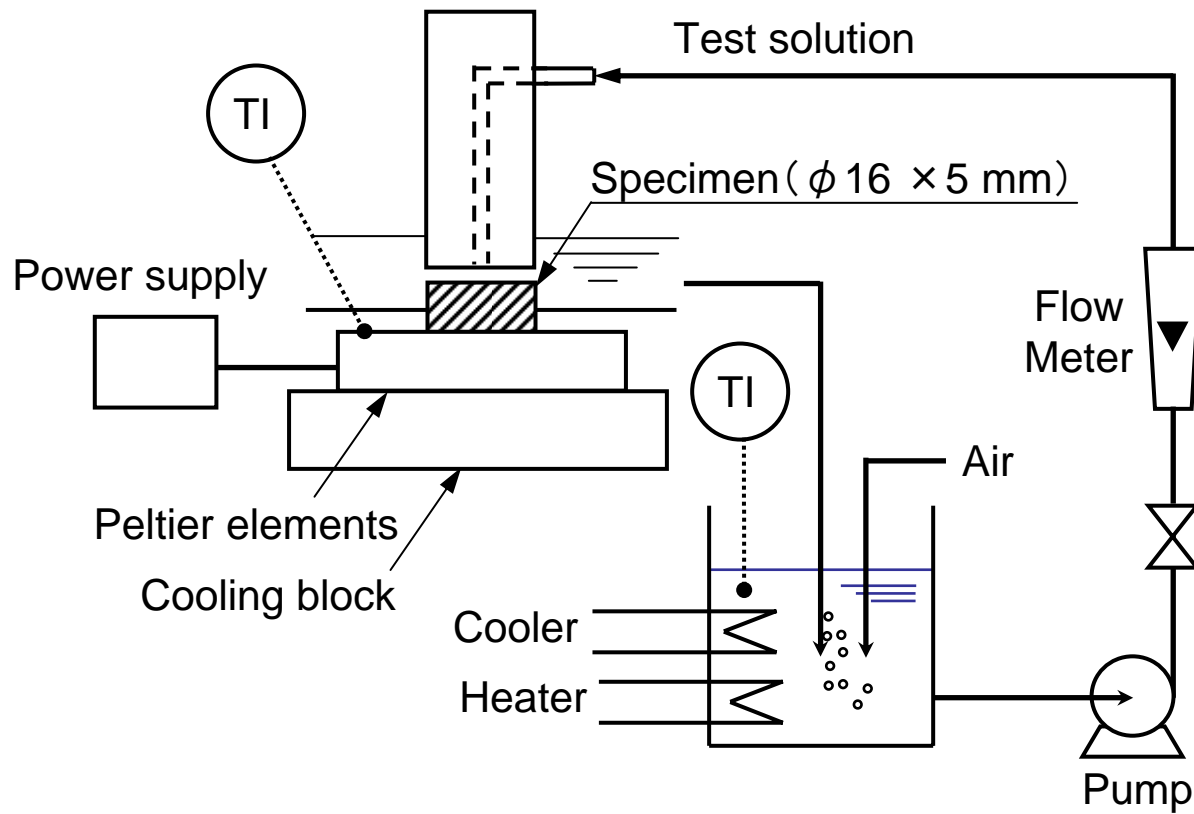


Fig. 1. Akihiro Yabuki et. al.

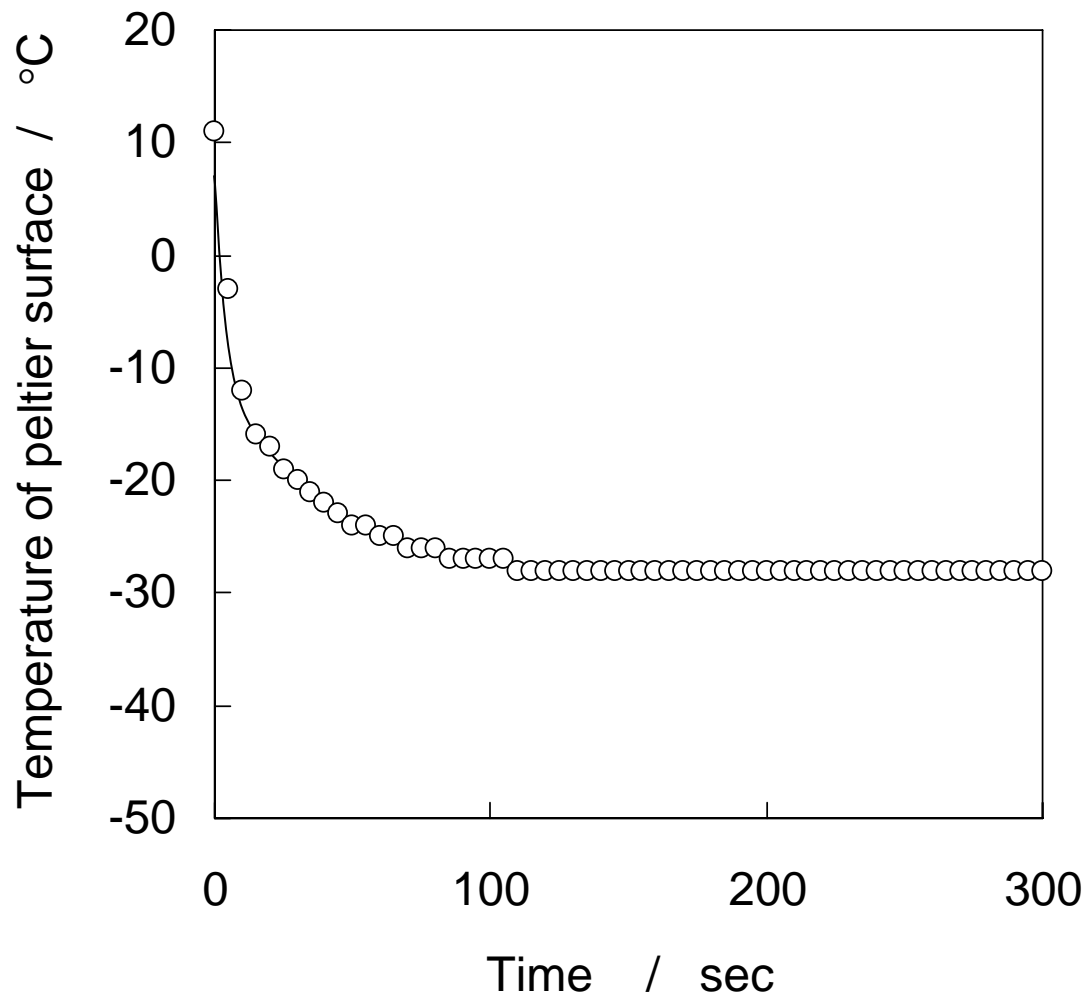


Fig. 2. Akihiro Yabuki et. al.

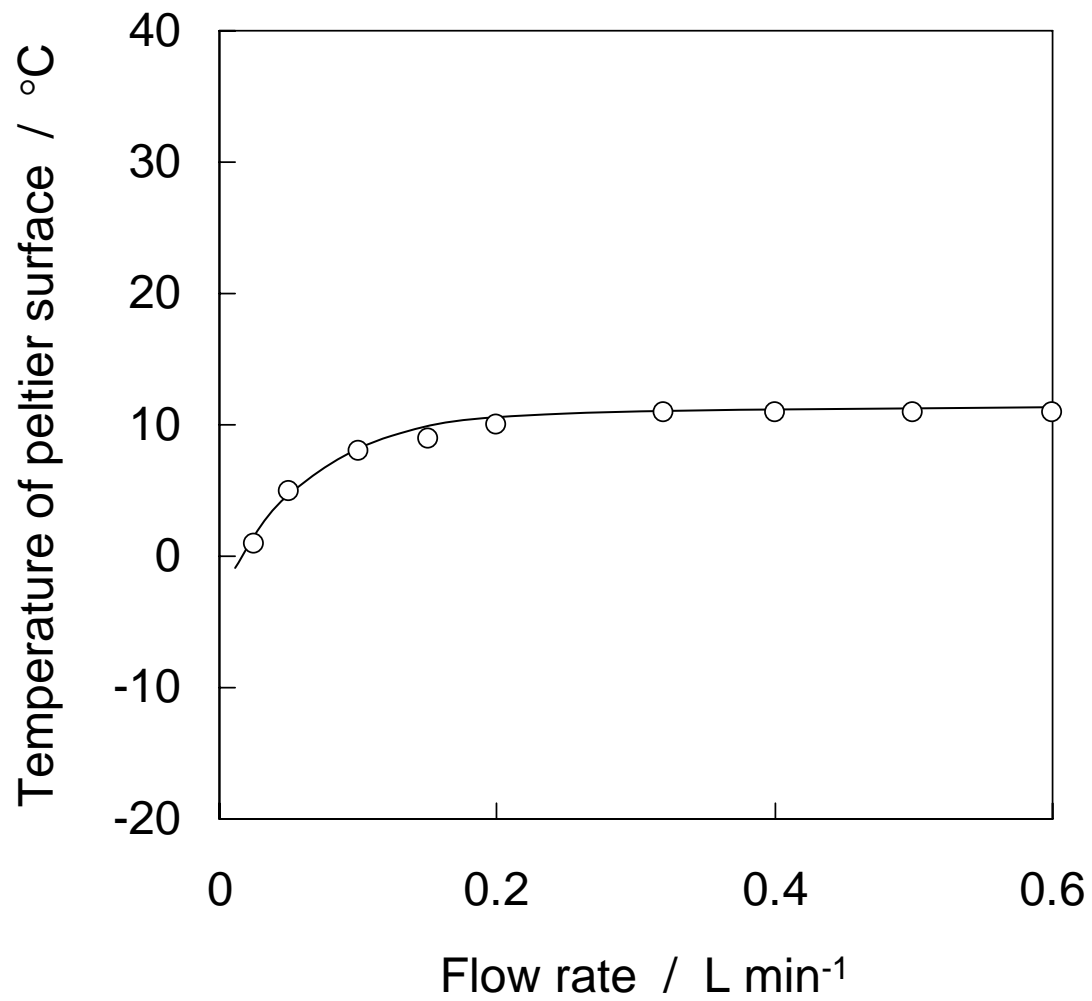


Fig. 3. Akihiro Yabuki et. al.

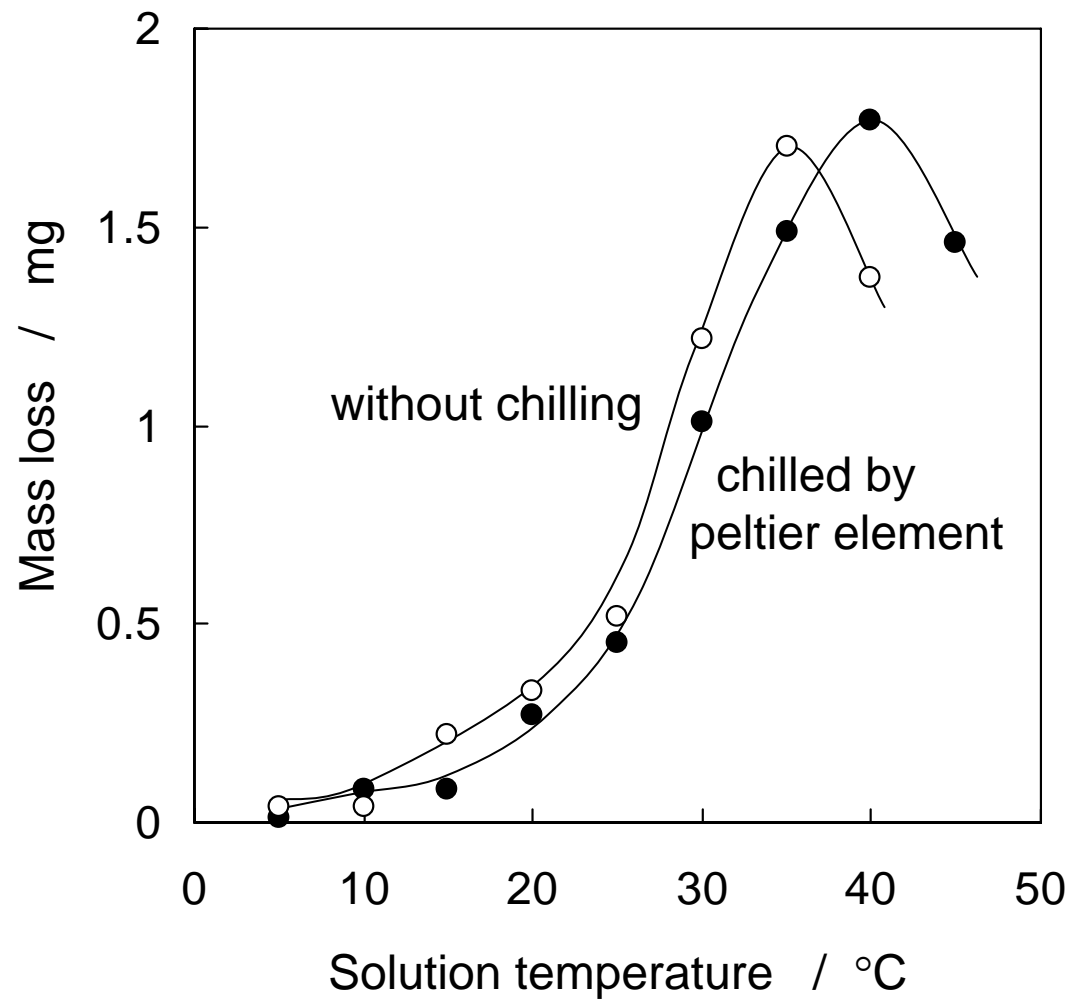


Fig. 4. Akihiro Yabuki et. al.

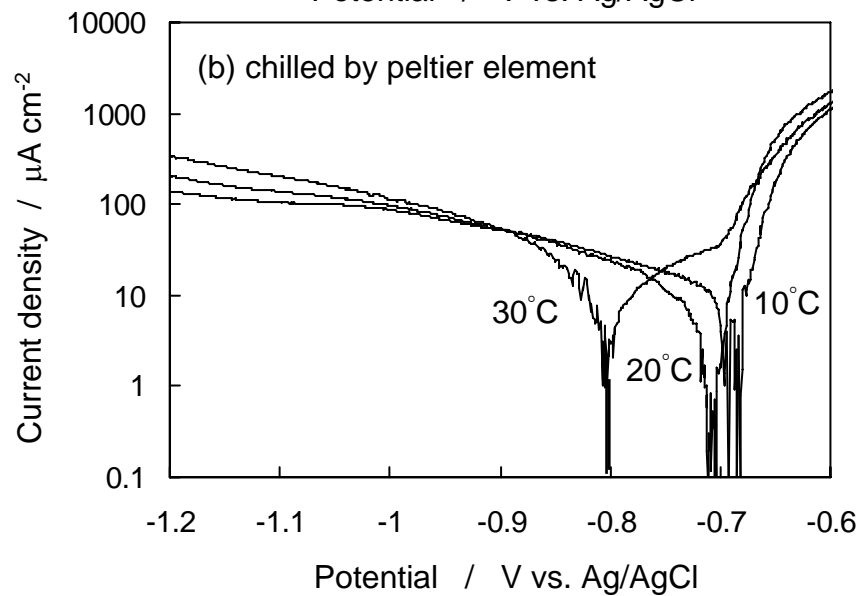
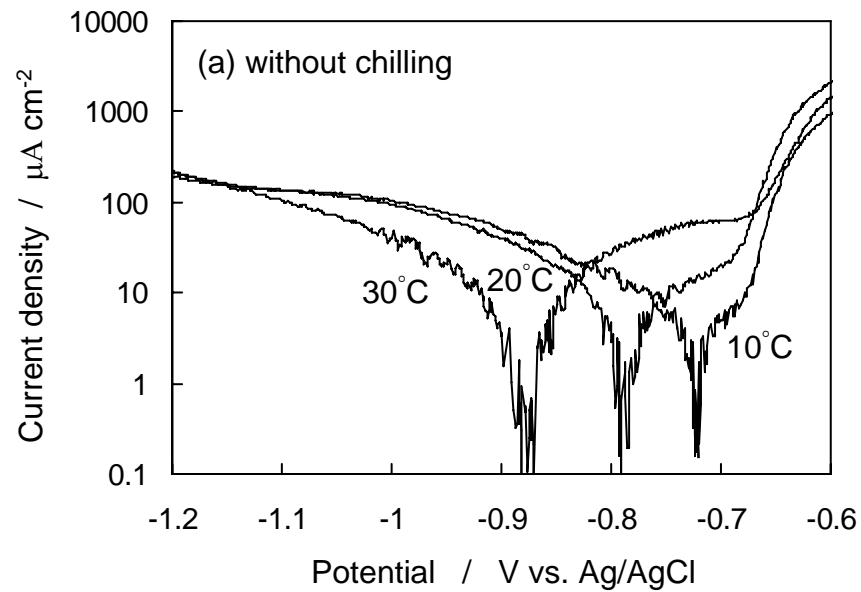


Fig. 5. Akihiro Yabuki et. al.

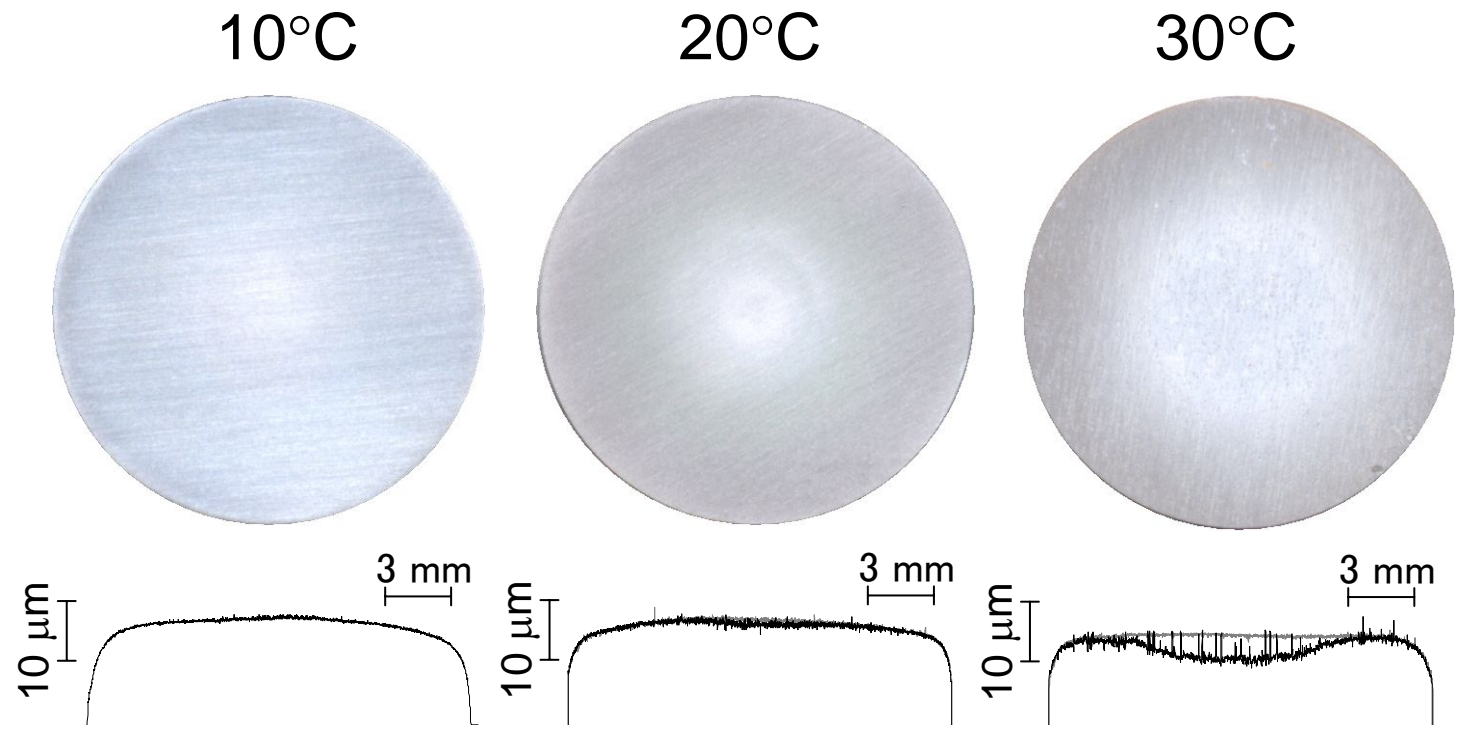


Fig. 6. Akihiro Yabuki et. al.

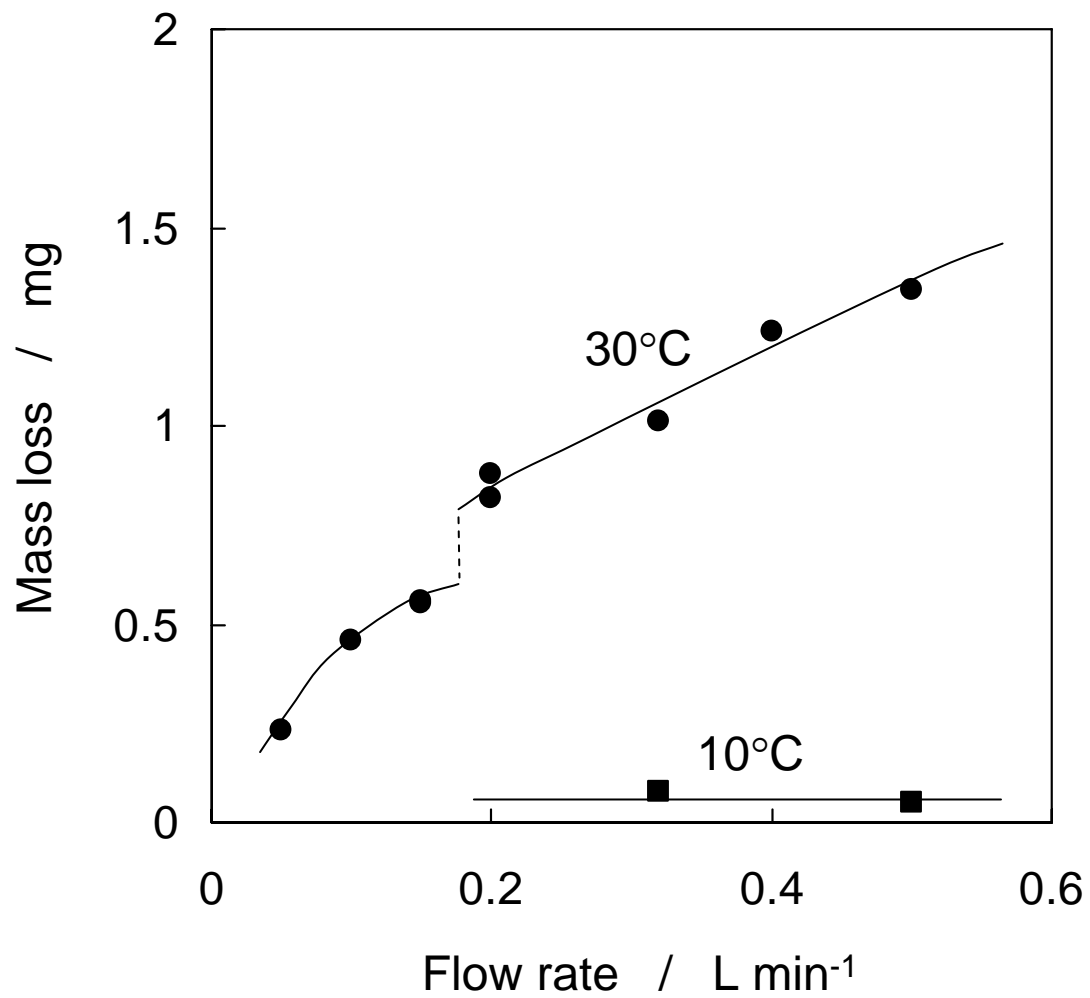


Fig. 7. Akihiro Yabuki et. al.

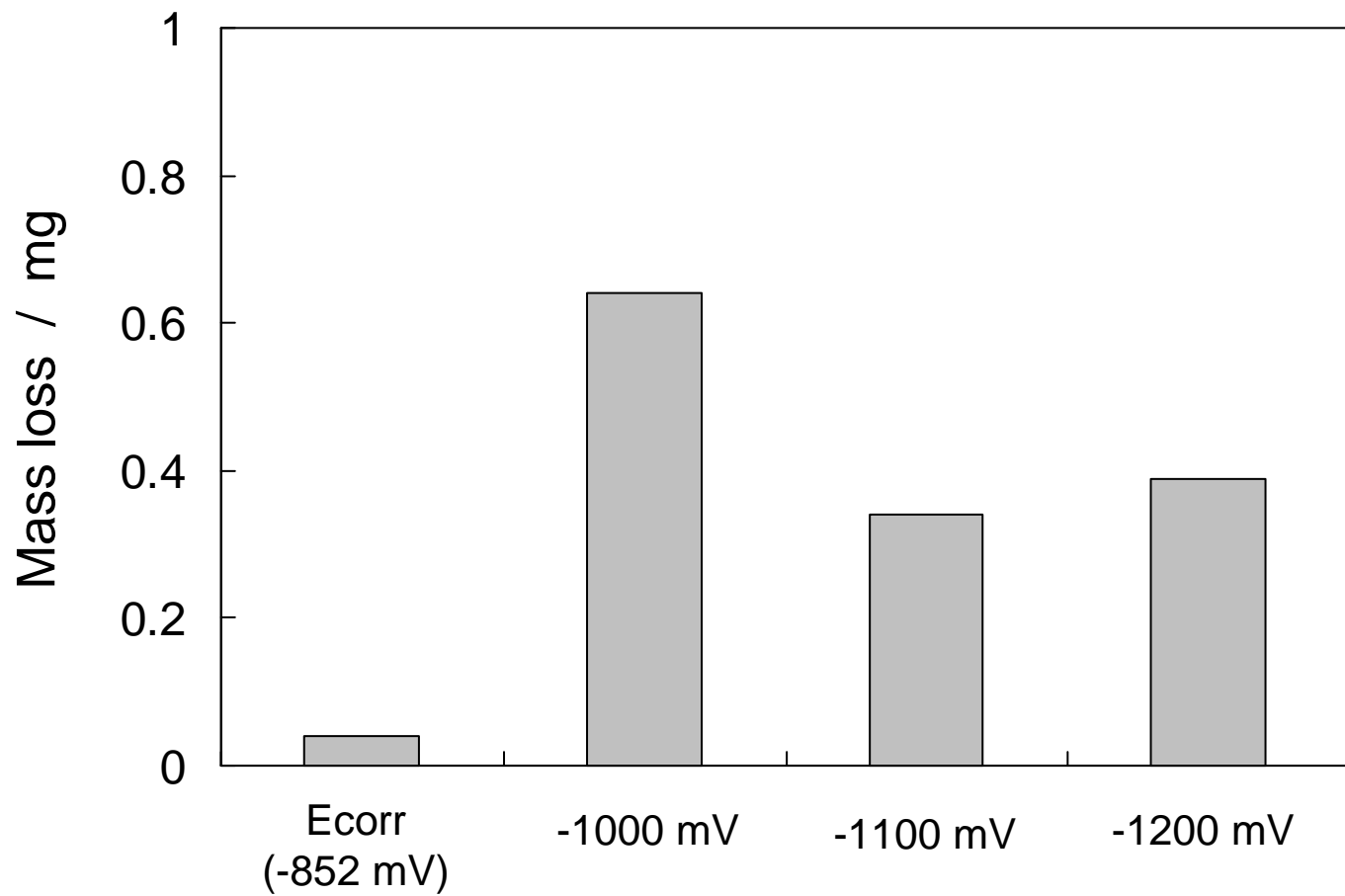


Fig. 8. Akihiro Yabuki et. al.

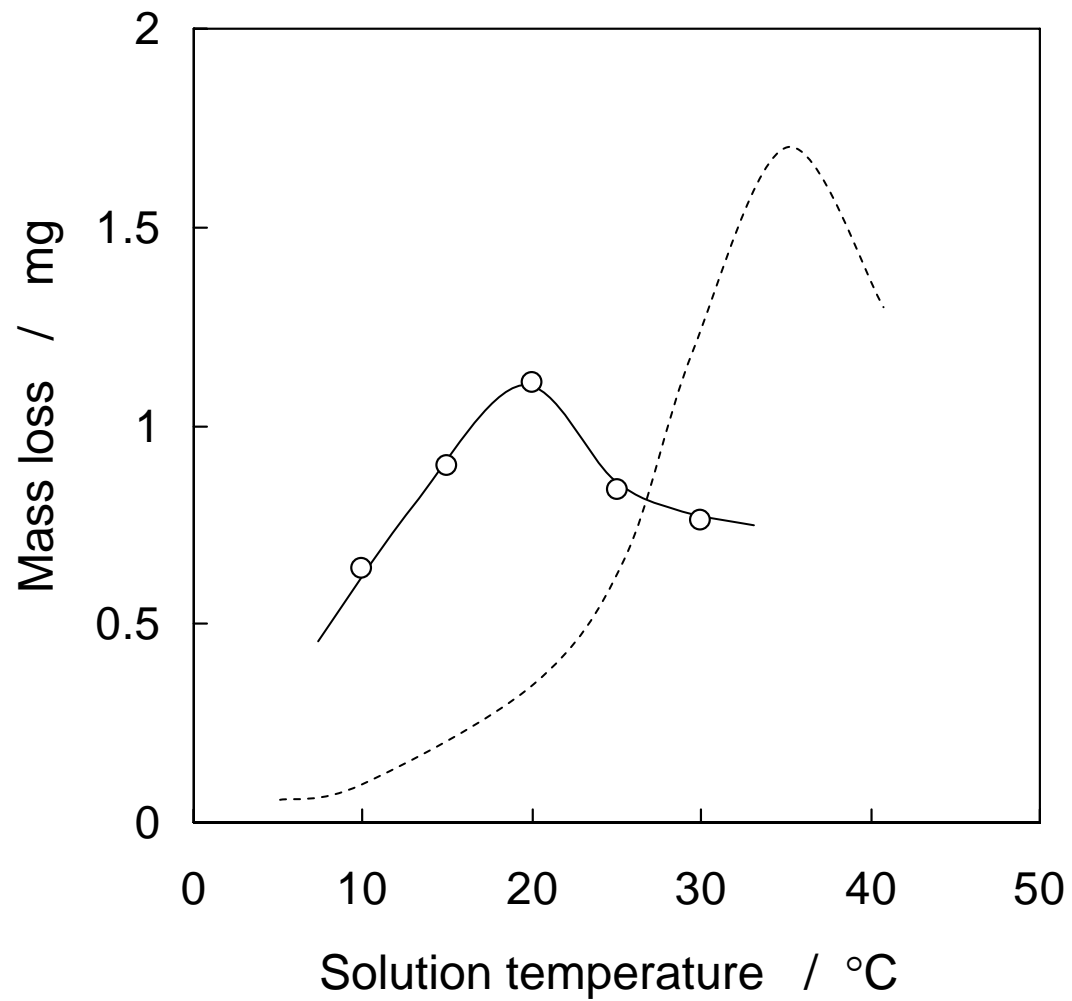


Fig. 9. Akihiro Yabuki et. al.

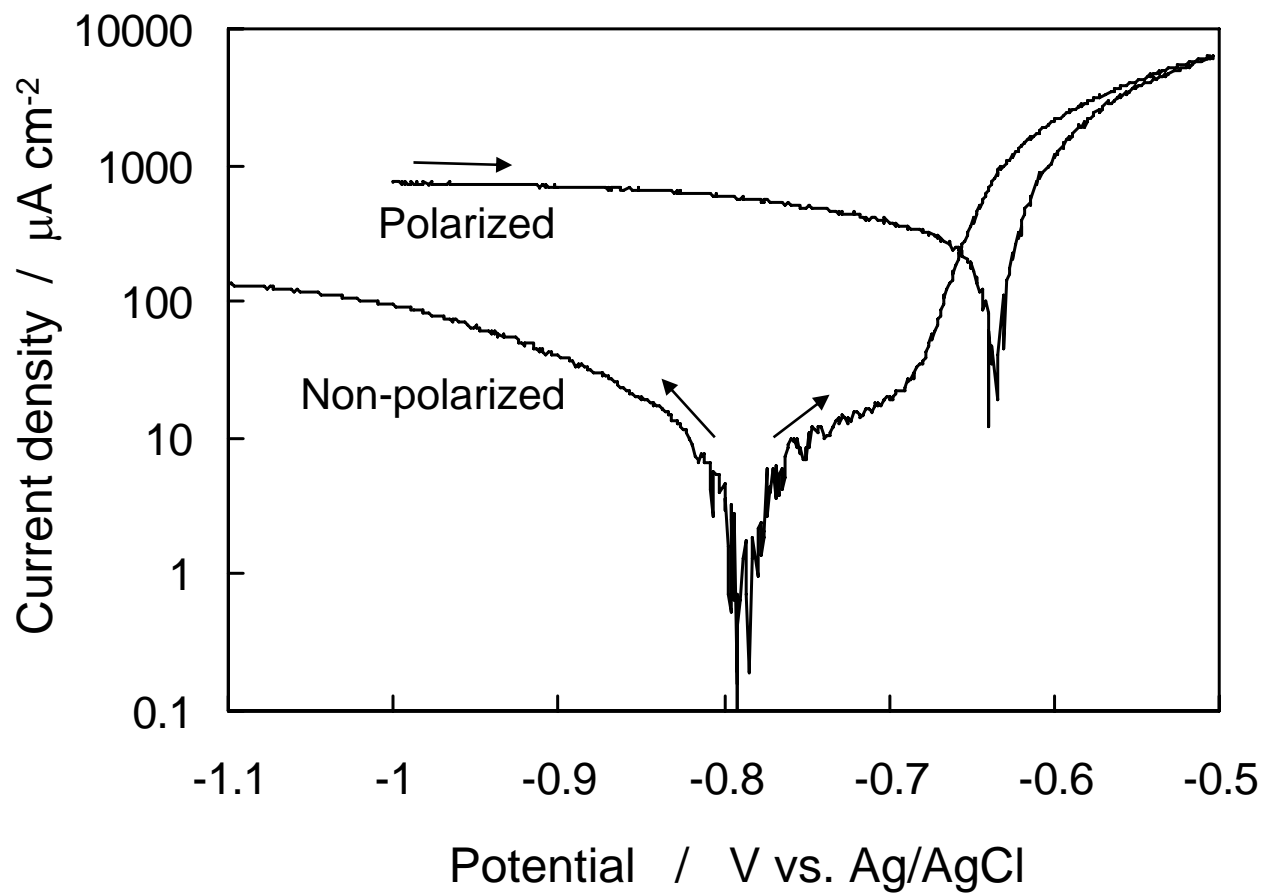


Fig. 10. Akihiro Yabuki et. al.

Table 1. Akihiro Yabuki et. al.

Al	Si	Fe	Cu	Mn	Mg	Cr	Zn	Ti
Base	0.10	0.25	0.02	0.87	4.51	0.08	0.01	0.02